Identification of a mitotic Rac-GEF, Trio, that counteracts MgcRacGAP function during cytokinesis

Aude Cannet[a], Susanne Schmidt[a], Bénédicte Delaval[b,*], and Anne Debant[a,*]
[a]Signaling and Cytoskeleton Dynamics Group and [b]Centrosome, Cilia and Pathology Group, CRBM-CNRS, University of Montpellier, 34293 Montpellier, France

ABSTRACT **The Rho GTPases RhoA and Rac1 function as master regulators of cytokinesis by controlling the actomyosin cytoskeleton. RhoA and Rac1 have to be respectively activated and inactivated at the division plane for cytokinesis to occur properly. The inactivation of Rac1 at the cleavage furrow is controlled by MgcRacGAP. However, the guanine-nucleotide exchange factor (GEF) that activates Rac1 during cell division remains unknown. Here, using a siRNA screening approach in HeLa cells, we identify Trio as a mitotic GEF of Rac1. We demonstrate that Trio controls Rac1 activation and subsequent F-actin remodeling in dividing cells. Moreover, Trio depletion specifically rescues the cytokinesis failure induced by MgcRacGAP depletion. Of importance, we demonstrate that this rescue is mediated by the Trio-Rac1 pathway, using GEF-dead mutants of Trio and a specific inhibitor of Rac1 activation by Trio. Overall this work identifies for the first time a GEF controlling Rac1 activation in dividing cells that counteracts MgcRacGAP function in cytokinesis.**

Monitoring Editor
Fred Chang
Columbia University

Received: Jun 25, 2014
Revised: Sep 17, 2014
Accepted: Oct 14, 2014

INTRODUCTION

During cell division, cells undergo dramatic changes in shape and adhesion that depend on efficient actin cytoskeleton remodeling. This process has to be locally and temporally regulated to accurately ensure cytokinesis, the final stage of cell division. The small GTPases Rac1 and RhoA play an essential role in this process by controlling F-actin cytoskeleton remodeling (Jaffe and Hall, 2005; Jordan and Canman, 2012). GTPases oscillate between an inactive, GDP-bound state and an active, GTP-bound state. They are activated by guanine-nucleotide exchange factors (GEFs), which stimulate the GDP-to-GTP exchange, whereas they are turned off by GTPase-activating proteins (GAPs), which catalyze the hydrolysis of GTP. RhoGEFs and RhoGAPs play a crucial role in controlling the regulation of the GTPases (Schmidt and Hall, 2002; Jaffe and Hall, 2005; Rossman *et al.*, 2005). RhoA is a positive regulator of cytokinesis specifically activated at the division plane, which promotes the assembly and constriction of the actomyosin network (Bement *et al.*, 2005; Yüce *et al.*, 2005). In contrast, Rac1 has been proposed to negatively regulate this process and has to be inactivated at the division plane for cytokinesis to occur properly (Yoshizaki *et al.*, 2003; Canman *et al.*, 2008; D'Avino and Glover, 2009; Bastos *et al.*, 2012). Indeed, expression of constitutively active Rac1 induces multinucleated cells, as expected for a negative regulator (Yoshizaki *et al.*, 2004), but disruption of Rac1 activity does not (Jantsch-Plunger *et al.*, 2000; Yoshizaki *et al.*, 2004; Canman *et al.*, 2008). A central spindle–localized GAP, MgcRacGAP, component of the centralspindlin complex, plays an essential role in this regulation. Indeed, recent studies from both mammalian cells and *Caenorhabditis elegans* embryos demonstrate that MgcRacGAP functions as a GAP of Rac1 at the cleavage furrow. MgcRacGAP controls Rac1 inactivation at the cleavage plane, and depletion of Rac1 or of Rac1 effectors can suppress the cytokinesis failure induced by MgcRacGAP depletion (Canman *et al.*, 2008; Bastos *et al.*, 2012). However, the RhoGEF controlling Rac1 activation in dividing cells has not yet been identified.

This article was published online ahead of print in MBoC in Press (http://www.molbiolcell.org/cgi/doi/10.1091/mbc.E14-06-1153) on October 29, 2014.

*These should be considered co–senior authors.

Address correspondence to: Anne Debant (anne.debant@crbm.cnrs.fr), Bénédicte Delaval (benedicte.delaval@crbm.cnrs.fr).

Abbreviations used: Dbl, diffuse B-cell lymphoma; GAP, GTPase-activating protein; GEF, guanine nucleotide exchange factor.

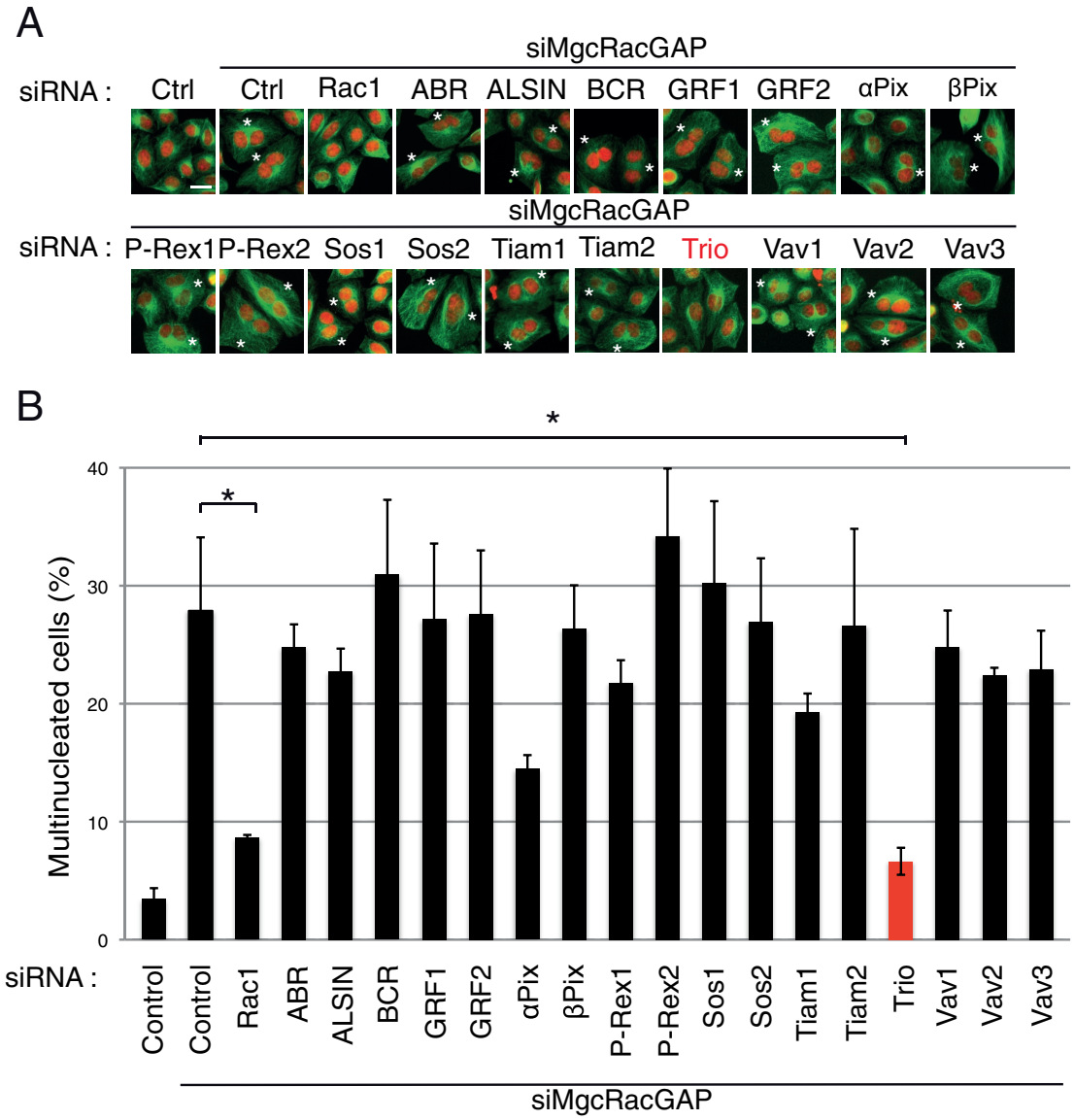

FIGURE 1: A siRNA screening approach identifies Trio as a potential GEF of Rac1 in dividing cells. HeLa cells were transfected with MgcRacGAP siRNA (siMgcRacGAP) in combination with control siRNA, Rac1 siRNA, or siRNAs targeting the indicated GEFs (SMART pools) and scored for the presence of multinucleated cells 48 h posttransfection. (A) Immunofluorescence of HeLa cells stained with DAPI (nuclei, red) and α-tubulin (green). Asterisks, multinucleated cells. Scale bar, 20 μm. (B) Quantification of the percentage of multinucleated cells. Five hundred cells were counted per experiment. Three independent experiments. Mean ± SEM. *$p < 0.02$.

RESULTS

A small interfering RNA screening approach in HeLa cells identifies Trio as a potential Rac1 GEF in dividing cells

To identify a RhoGEF regulating Rac1 activity in dividing cells, we performed a small interfering RNA (siRNA) screening approach in HeLa cells using SMARTpool siRNA oligonucleotides. Seventeen Rac GEFs belonging to the diffuse B-cell lymphoma (Dbl) family (Rossman *et al.*, 2005) were depleted by siRNA alone or in combination with MgcRacGAP siRNAs in order to identify the ones able to rescue the cytokinesis failure induced by MgcRacGAP depletion (Figure 1 and Supplemental Figure S1). Of note, depletion of RacGEFs alone did not lead to a significant increase in the number of multinucleated cells (unpublished data). As previously described, 48 h after siRNA treatment, MgcRacGAP depletion resulted in the appearance of multinucleated cells, consistent with cytokinesis failure (Figure 1 and Supplemental Figure S1; Bastos *et al.*, 2012). Codepletion of MgcRacGAP and Rac1 efficiently rescued the number of multinucleated cells (Figure 1), confirming that MgcRacGAP is acting as a GAP for Rac1 at the cleavage furrow of HeLa cells (Bastos *et al.*, 2012). Of importance, codepletion of MgcRacGAP and Trio, a GEF characterized primarily for its role in axon outgrowth and guidance via RhoG/Rac1 activation (Steven *et al.*, 1998; Bateman *et al.*, 2000; Newsome *et al.*, 2000; Estrach *et al.*, 2002; Briançon-Marjollet *et al.*, 2008; DeGeer *et al.*, 2013), resulted in a strong decrease in the number of multinucleated cells (Figure 1). This result indicated that Trio depletion could rescue the cytokinesis failure induced by MgcRacGAP depletion. Of note, codepletion of MgcRacGAP and αPix also resulted in the decrease of multinucleated cells, but to a lower extent than Trio depletion. Of interest, the extent of the rescue induced by Trio depletion was similar to the one obtained with the codepletion

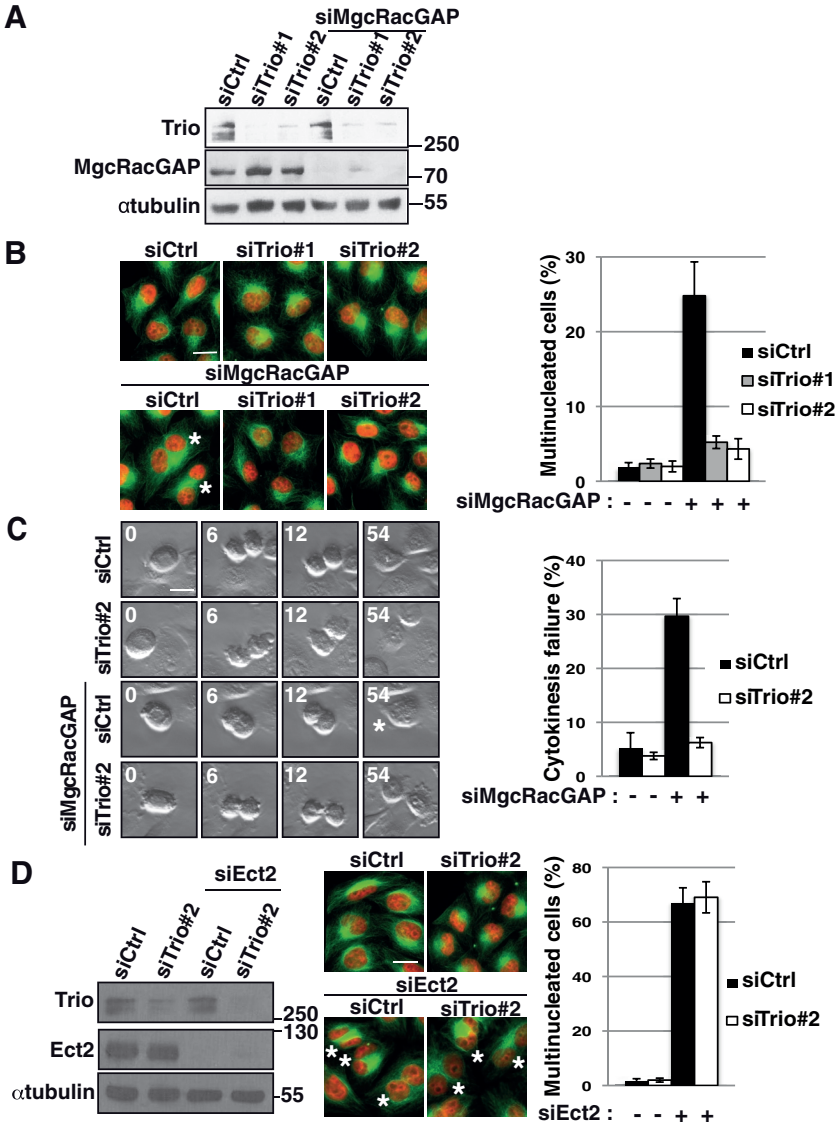

FIGURE 2: Trio depletion rescues the cytokinesis failure induced by the depletion of MgcRacGAP. (A) Western blot showing the amount of Trio and MgcRacGAP 30 h after siRNA transfection. siRNA conditions include control siRNA (siCtrl) and two independent siRNAs against Trio (siTrio#1, siTrio#2) alone or in combination with MgcRacGAP siRNA (siMgcRacGAP). α-Tubulin, loading control. Molecular weight is indicated in kilodaltons. (B) Immunofluorescence of HeLa cells stained with DAPI (nuclei, red) and α-tubulin (green) to visualize multinucleated cells upon MgcRacGAP depletion. siRNA conditions, as indicated. Asterisks, multinucleated cells. Scale bar, 20 μm. Graph shows quantification of the percentage of multinucleated cells. $n = 500$ cells; three independent experiments. Mean ± SEM. (C) Frames from movies showing cells undergoing cytokinesis. Cytokinesis failure is observed in MgcRacGAP siRNA–treated cells but not in control, Trio2, or Trio2/MgcRacGAP siRNA–treated cells. Asterisks, multinucleated cells. Time (minutes) is indicated in the upper left corner. Scale bar, 20 μm. Graph shows quantification of the percentage of dividing cells undergoing cytokinesis failure at the end of the first division after siRNA transfection. $n > 30$ cells/experiment; three independent experiments. Mean ± SEM. (D) Western blot showing the amount of Trio and Ect2 30 h after siRNA transfection. siRNA conditions include control siRNA (siCtrl) and Trio siRNA alone or in combination with Ect2 siRNA (siEct2). α-Tubulin, loading control. Molecular weight is indicated in kilodaltons. Immunofluorescence of HeLa cells stained with DAPI (nuclei, red) and α-tubulin (green) to visualize multinucleated cells upon Ect2 depletion. siRNA conditions, as indicated. Asterisks, multinucleated cells. Scale bar, 20 μm. Graph shows quantification of the percentage of multinucleated cells. $n = 500$ cells; three independent experiments. Mean ± SEM.

of Rac1 (Figure 1). Even if the involvement of other GEFs activating Rac1 during cell division cannot be excluded, our screening approach identifies Trio as a major GEF of Rac1 in dividing cells.

To confirm that Trio can function in dividing cells, we monitored Trio expression by performing Western blot analyses and immunofluorescence studies (Supplemental Figure S2, A and B). Trio was expressed in dividing cells, and the level of the protein remained constant during the cell cycle (Supplemental Figure S2A). In dividing cells, endogenous Trio was mostly diffusely expressed (Supplemental Figure S2B). It did not specifically concentrate at the cleavage furrow but appeared enriched in actin-rich structures (Supplemental Figure S2B). Of importance, this staining was lost upon Trio depletion by siRNA, demonstrating the specificity of the endogenous localization (Supplemental Figure S2B, bottom).

To confirm that Trio depletion could rescue the cytokinesis failure induced by MgcRacGAP depletion, we used two independent siRNAs to deplete Trio in combination with MgcRacGAP siRNA in HeLa cells. Protein depletion was controlled by Western blot analysis and immunofluorescence staining (Figure 2A and Supplemental Figure S2C). Of importance, both Trio siRNAs efficiently rescued the number of multinucleated cells induced by MgcRacGAP depletion, demonstrating that the observed phenotype was indeed specific to Trio depletion (Figure 2B).

To further demonstrate that the rescue observed in Trio/MgcRacGAP depleted cells was specifically due to the rescue of cytokinesis failure, we performed live imaging to directly monitor dividing cells going through cytokinesis (Figure 2C and Figure 2 Videos S1–S4). Cells were monitored as they entered cell division and scored for successful or failed cytokinesis. Upon MgcRacGAP depletion, 29.7% of cells failed cytokinesis, leading to the appearance of multinucleated cells (Figure 2C). Strikingly, only 6.2% of Trio- and MgcRacGAP-codepleted cells failed cytokinesis, showing that the depletion of Trio indeed rescued the cytokinesis failure induced by the loss of MgcRacGAP (Figure 2C and Figure 2 Videos S1–S4). Of note, Trio depletion alone led to a slight change in cell morphology but did not induce any significant cytokinesis failure (Figure 2, B and C, and Figure 2 Videos S1 and S2), as previously reported for Rac1 depletion (Jantsch-Plunger *et al.*, 2000; Canman *et al.*, 2008; D'Avino and Glover, 2009).

To determine whether the rescue observed after Trio depletion was specific to the cytokinesis failure induced by MgcRacGAP depletion, we tested whether Trio depletion was able to rescue the cytokinesis failure induced by the depletion of Ect2 a major activator of the GTPase RhoA during cytokinesis (Yüce *et al.*, 2005). Of

interest, Trio depletion did not rescue the cytokinesis failure induced by Ect-2 siRNA depletion (Figure 2D). Taken together, these results demonstrate that Trio depletion can specifically rescue the cytokinesis failure induced by MgcRacGAP depletion. Given that MgcRacGAP was described to be essential for Rac1 inactivation in cytokinesis (Canman *et al.*, 2008; Bastos *et al.*, 2012), this also suggests that Trio could rescue the cytokinesis failure induced by MgcRacGAP depletion by decreasing Rac1 activity. This therefore suggests that Trio could be a GEF of Rac1 in dividing cells.

Trio functions as a GEF of Rac1 during cell division

To directly test whether Trio could function as a GEF of Rac1 in dividing cells, the amount of activated Rac1 was monitored by pull-down assay in synchronized mitotic cells. Compared to control siRNA–treated cells, Trio depletion reduced by half the amount of activated Rac1 in mitotic cells (Figure 3A), showing that Trio activates Rac1 in mitosis. Strikingly, Trio depletion (Figure 3B) led to defects in F-actin cytoskeleton remodeling in both interphase (unpublished data) and dividing cells (Figure 3C). More specifically, in anaphase cells, the F-actin staining at the cortex was significantly reduced in Trio-depleted cells compared with control cells (Figure 3C, MP). This decrease in F-actin staining was particularly obvious at the bottom plane (Figure 3, C–E, BP and inset), where cells are in contact with the substrate. Of interest, Trio depletion phenocopied the depletion of Rac1, consistent with a role for the Trio-Rac1 pathway in controlling F-actin remodeling in dividing cells (Figure 3, B–E). Trio depletion also phenocopied the depletion of actin-related protein 3 (Arp3; Figure 3, B–E), a component of the Arp2/3 complex whose depletion disrupts the Arp2/3 complex (Steffen *et al.*, 2006). Arp2/3 is known to nucleate branched actin filaments downstream of Rac1 (Pollard, 2007). Taken together, these results suggest that Trio could control F-actin remodeling during cell division by controlling the Rac1-Arp2/3 pathway.

To confirm that Trio activates Rac1 to control F-actin remodeling in dividing cells, we performed rescue experiments using the GEFD1 domain of Trio (green fluorescent protein [GFP]–DH1PH1; Figure 4, A–C, and Supplemental Figure S3). This domain was previously shown to strongly activate Rac1 (Bellanger *et al.*, 1998). Expression of GFP-DH1PH1, insensitive to Trio siRNAs (Supplemental Figure S3), efficiently rescued the F-actin cytoskeleton remodeling defects observed in Trio-depleted anaphase cells (Figure 4, A–C). To demonstrate further the involvement of the Trio-Rac1 pathway in controlling F-actin remodeling in dividing cells, we used ITX3, a specific inhibitor of Rac1 activation by Trio (Bouquier *et al.*, 2009). ITX3 treatment phenocopied Trio depletion (Figure 4D). Taken together, these results demonstrate that Trio functions as a GEF of Rac1 during cell division and that the Trio-Rac1-Arp2/3 pathway is important to control F-actin cytoskeleton remodeling in dividing cells.

Inhibition of the Trio-Rac1 pathway specifically rescues the cytokinesis failure induced by MgcRacGAP depletion

Recent studies from both mammalian cells and *C. elegans* embryos demonstrate that MgcRacGAP is essential at the cleavage furrow to inactivate Rac1 at the anaphase–telophase transition to allow for proper cytokinesis to occur (Canman *et al.*, 2008; Bastos *et al.*, 2012). In *C. elegans* embryos, Rac1 inhibition at the division plane is important to prevent Arp2/3 complex activation, and Arp2/3 complex disruption rescues the cytokinesis failure induced by MgcRacGAP depletion (Canman *et al.*, 2008). In agreement with these results, Arp3 depletion by siRNA in HeLa cells, which disrupts the Arp2/3 complex (Steffen *et al.*, 2006), rescued the number of multinucleated cells induced by MgcRacGAP depletion (Supplemental Figure S4A).

To investigate directly whether Trio depletion rescues the cytokinesis failure induced by MgcRacGAP depletion by controlling Rac1 activation, we examined whether the increase in multinucleated cells induced by MgcRacGAP depletion could be suppressed using ITX3, the specific inhibitor of Rac1 activation by Trio (Bouquier *et al.*, 2009). siRNA depletion of MgcRacGAP upon ITX3 treatment was controlled by Western blot analysis and immunofluorescence staining (Figure 5A and Supplemental Figure S4B). Strikingly, ITX3 treatment rescued the number of multinucleated cells induced by MgcRacGAP depletion (Figure 5B). This demonstrates that inhibition of Rac1 activation by Trio rescues the cytokinesis failure induced by MgcRacGAP depletion by decreasing Rac1 activity.

To further confirm that Trio depletion rescued the cytokinesis failure induced by MgcRacGAP depletion by controlling Rac1 activity, we expressed siRNA-resistant forms of wt Trio or GEF-dead mutants of Trio (Supplemental Figure S3) and monitored whether this could suppress the rescue (Figure 5C and Supplemental Figure S4C). Because Trio harbors two GEF domains activating, respectively, the GTPase Rac1/RhoG (GEFD1) and RhoA (GEFD2), we used a GEFD1-dead mutant of Trio unable to activate Rac1/RhoG (GFP-D1d) and a GEFD2-dead mutant of Trio unable to activate RhoA (GFP-D2d; Supplemental Figure S4C). Of note, expression of Trio or of Trio mutants per se did not induce multinucleated cells (unpublished data). As previously shown, Trio depletion rescued the cytokinesis failure induced by MgcRacGAP depletion (Figures 1 and 2). Of importance, the rescue was partially suppressed by expressing GFP-Trio wt or GFP-D2d but not by expressing GFP-D1d (Figure 5C). This confirms the involvement of the Trio-Rac1 pathway in the rescue phenotype and indicates that RhoA activation by Trio is not involved in this process. Overall these results demonstrate that Trio depletion specifically rescues the cytokinesis failure induced by MgcRacGAP depletion by decreasing Rac1 activity.

DISCUSSION

Rac1 negatively regulates the assembly and constriction of the contractile ring during cytokinesis. This process is regulated by a GAP, MgcRacGAP, which is essential to inhibit Rac1 activation at the cleavage furrow (Canman *et al.*, 2008; Bastos *et al.*, 2012). Collectively our results show that Trio, known mainly for its role in neuronal development, plays an unexpected role in dividing cells, where it controls the activation of the GTPase Rac1 and subsequent F-actin cytoskeleton remodeling. Moreover, Trio depletion or specific inactivation of the Trio-Rac1 pathway rescues the cytokinesis failure induced by MgcRacGAP depletion in HeLa cells. On the basis of these observations, we propose a model in which Trio functions as a GEF of Rac1 during cell division. Trio, which is expressed throughout the cell cycle, activates Rac1 to control F-actin cytoskeleton remodeling at the cell cortex of dividing cells. As previously described, MgcRacGAP is up-regulated in mitosis and targeted to the cleavage furrow to specifically inhibit Rac1 at the cleavage plane during cytokinesis (Hirose *et al.*, 2001; Canman *et al.*, 2008; Seguin *et al.*, 2009; Bastos *et al.*, 2012). MgcRacGAP therefore counteracts the action of Trio by locally and temporally inhibiting Rac1 activation at the division plane, subsequently ensuring accurate cytokinesis (Figure 6).

In this study, we identify for the first time a GEF of Rac1 in dividing cells, Trio, using a siRNA screening approach for GEFs belonging to the Dbl family. Trio is a complex protein harboring two GEF domains, activating, respectively, RhoG/Rac1 and RhoA (Bellanger *et al.*, 1998). Taken together, our experiments show that the rescue by Trio depletion of the cytokinesis failure induced by MgcRacGAP

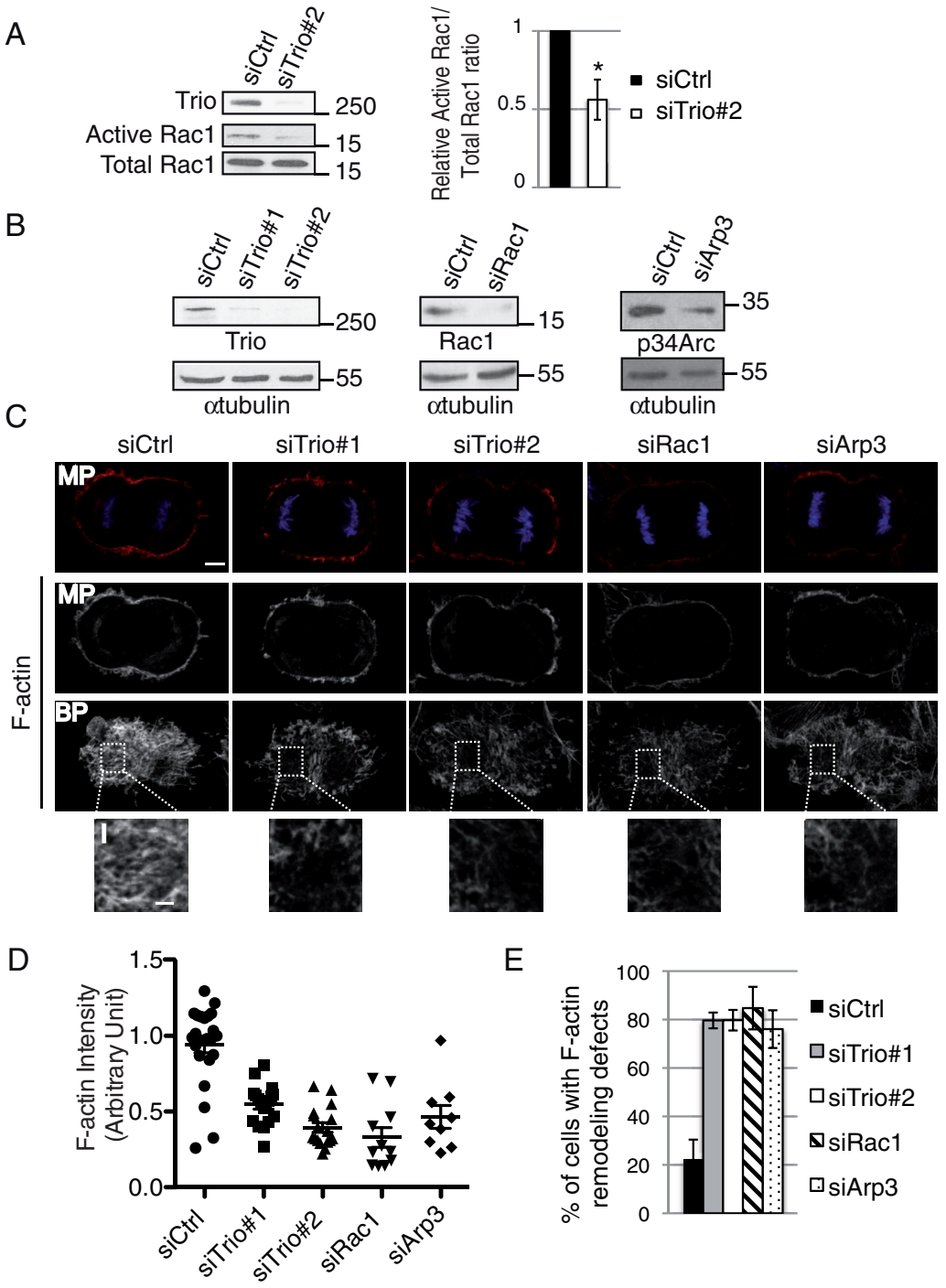

FIGURE 3: Trio depletion decreases Rac1 activity in dividing cells and leads to F-actin remodeling defects. (A) Quantification of GTP-bound Rac1 in control and Trio#2 siRNA–treated mitotic cells. Western blot showing the amount of Rac1 bound to GST-CRIB (Active Rac1) and the total level of Rac1 expression (Total Rac1). Immunoblot, anti-Rac1 antibody. Molecular weight is indicated in kilodaltons. Histogram (right), relative Active Rac1/Total Rac1 ratio. Mitotic index, 60%. Three independent experiments. Mean ± SEM. *$p < 0.01$. (B) Western blot showing the amount of Trio, Rac1, or p34-Arc. p34-Arc is used to control for Arp2/3 complex disruption. siRNA conditions include control, Trio#1, Trio#2, Rac1, or Arp3. α-Tubulin, loading control. Molecular weight is indicated in kilodaltons. (C) HeLa cells were transfected with control siRNA, Trio#1 siRNA, Trio#2 siRNA, Rac1 siRNA, or Arp3 siRNA. HeLa cells were stained with rhodamine-phalloidin to monitor the F-actin cytoskeleton (red) and DAPI (DNA, blue) to identify anaphase cells. Middle planes (MPs) and bottom planes (BPs) are shown to visualize actin remodeling defects. *Z*-stack maximum projection, 0881 µm. Scale bar, 5 µm; inset, 2 µm. (D) Graph showing the average F-actin intensity (bottom single plane) in each condition. Data from three independent experiments were pooled, and the actin intensity for each condition was normalized to the average intensity in control cells. Mean ± SEM. For all siRNA conditions compared with control siRNA, *$p < 00001$. (E) Graph showing the percentage of cells with F-actin remodeling defects. $n > 30$ anaphase cells; three independent experiments. Mean ± SEM.

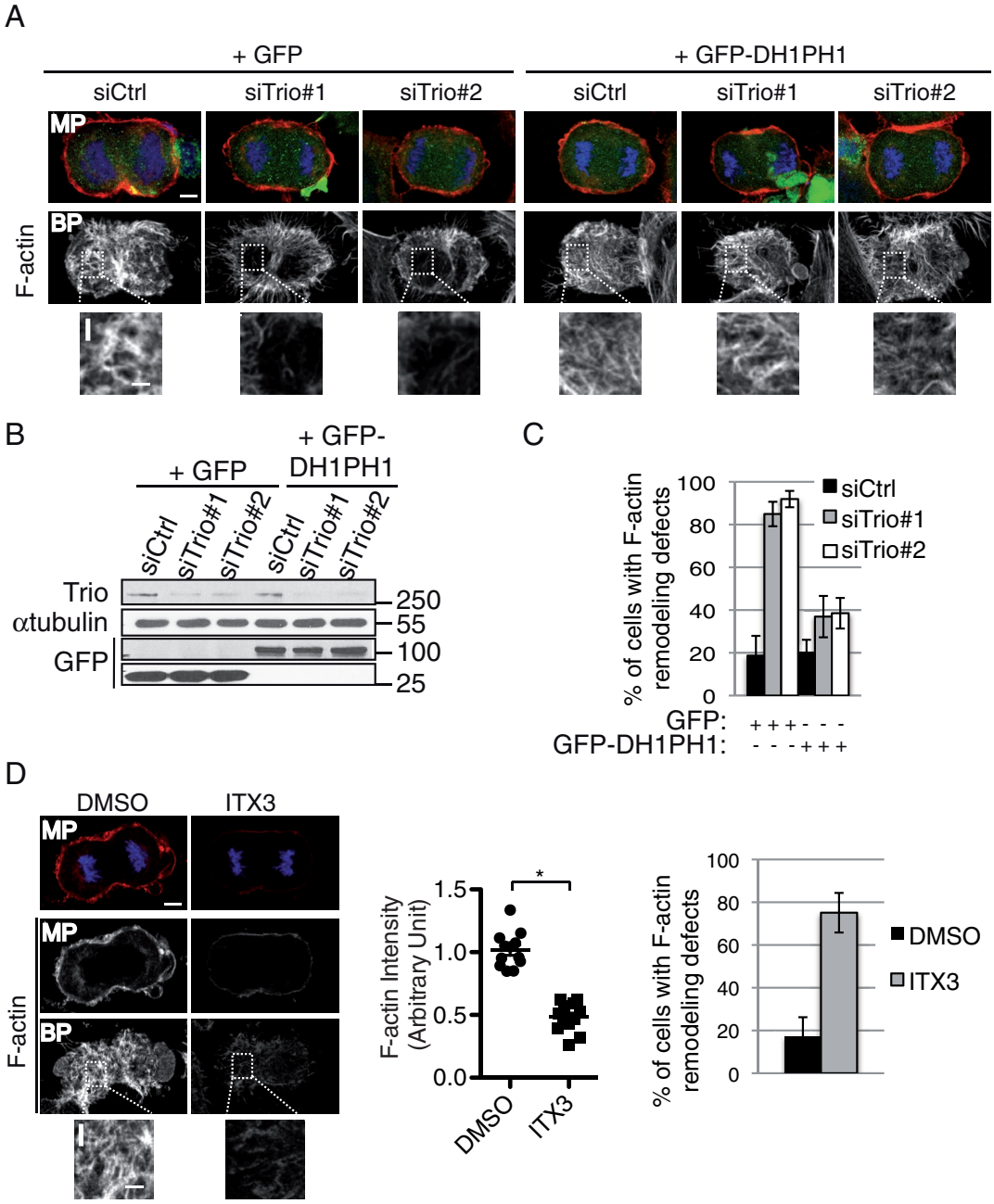

FIGURE 4: The Trio-Rac1 pathway is important to control F-actin remodeling in dividing cells. (A) Rescue experiment performed by transfecting HeLa cells with GFP or GFP-DH1PH1 (domain of Trio known to strongly activate Rac1) and Ctrl or Trio siRNAs as indicated. Cells were stained with rhodamine-phalloidin (actin, red) and DAPI (DNA, blue) to monitor F-actin remodeling defects. Middle planes (MPs) and bottom planes are shown. *Z*-stack maximum projection, 0881 µm. Scale bar, 5 µm; inset, 2 µm. (B) Western blot showing the amount of Trio and GFP or GFP-DH1-PH1. α-Tubulin, loading control. Molecular weight is indicated in kilodaltons. (C) Graph showing the percentage of cells with F-actin remodeling defects at the bottom plane. $n > 30$ anaphase cells/condition; three independent experiments. Mean ± SEM. (D) HeLa cells were treated with DMSO or ITX3 and stained with rhodamine-phalloidin to monitor the F-actin cytoskeleton (red) and DAPI (DNA, blue) to identify anaphase cells. Middle planes (MPs) and bottom planes (BPs) are shown to visualize actin remodeling defects. *Z*-stack maximum projection, 0881 µm. Scale bar, 5 µm; inset, 2 µm. Graph (middle) showing the average F-actin intensity (bottom single plane) in each condition. Data from three independent experiments were pooled, and the actin intensity for each condition was normalized to the average intensity in control cells. Mean ± SEM. *$p < 00001$. Graph (far right) shows the percentage of cells with F-actin remodeling defects. $n > 30$ anaphase cells; three independent experiments. Mean ± SEM.

depletion is due to a decrease in Rac1 activity. This result is consistent with the fact that previously described functions of Trio, such as neuronal development, migration, or invasion in mammalian cells, are also mediated by the activation of the RhoG/Rac1 pathway by Trio (Blangy *et al.*, 2000; Estrach *et al.*, 2002; Briançon-Marjollet *et al.*, 2008; Li *et al.*, 2011; van Rijssel *et al.*, 2012; Moshfegh *et al.*, 2014). Even if the involvement of other GEFs activating Rac1 or GEFs functioning as Rac1 effectors in dividing

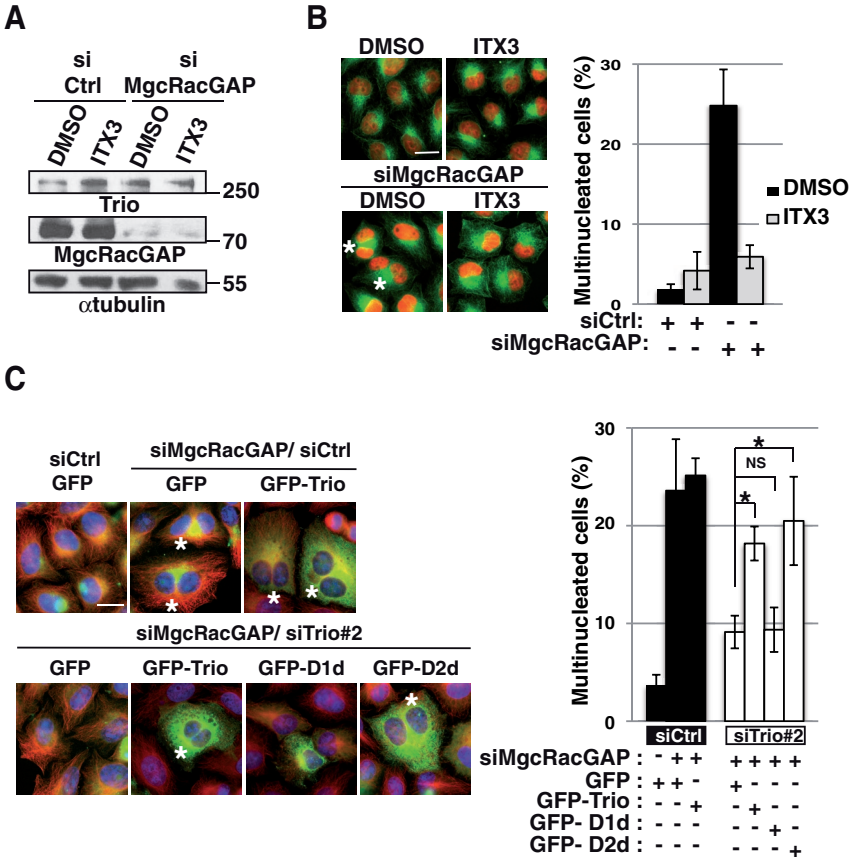

FIGURE 5: Inhibition of Rac1 activation by Trio rescues the cytokinesis failure induced by MgcRacGAP depletion. (A) HeLa cells were treated for 24 h with DMSO or ITX3 alone or in combination with MgcRacGAP siRNA. Western blot showing the amount of Trio and MgcRacGAP. α-Tubulin, loading control. Molecular weight is indicated in kilodaltons. (B) Immunofluorescence of HeLa cells stained with DAPI (nuclei, red) and α-tubulin (green) to monitor the presence of multinucleated cells after MgcRacGAP depletion upon DMSO or ITX3 treatments. Asterisks, multinucleated cells. Scale bar, 20 μm. Graph shows the quantification of the percentage of multinucleated cells. $n = 500$ cells; three independent experiments. Mean ± SEM. (C) Immunofluorescence of HeLa cells (left) cotransfected with MgcRacGAP siRNA and Ctrl or Trio siRNAs. GFP, GFP-Trio siRNA resistant, GFP-D1d siRNA resistant (GEFD1 dead mutant of Trio unable to activate Rac1/RhoG), or GFP-D2d siRNA resistant (GEFD2 dead mutant of Trio unable to activate RhoA) was transfected together with the indicated siRNA to monitor which mutant form of Trio can suppress the rescue. HeLa cells were stained with DAPI (nuclei, blue) and α-tubulin (red) to monitor multinucleated cells. Asterisks, multinucleated cells. Scale bar, 20 μm. Graph shows the quantification of the percentage of multinucleated cells after codepletion of Trio and MgcRacGAP and expression of mutant forms of Trio. Five hundred cells were counted per experiment; three independent experiments. Mean ± SEM. *$p < 0.05$.

cells cannot be excluded, our screening approach identifies Trio as a major GEF controlling Rac1 activation in dividing cells. Of note, depletion of RhoG, the other target of the first GEF domain of Trio, did not rescue the depletion of MgcRacGAP, indicating that the rescue is mediated by Rac1 and not by RhoG (unpublished data), as previously reported in *C. elegans* (Canman *et al.*, 2008).

By identifying a novel mitotic regulator of Rac1 important for F-actin cytoskeleton remodeling, this work improves our understanding of Rac1 regulation in dividing cells. Rac1, which is activated by Trio at the cell cortex of dividing cells, must be specifically inhibited at the division plane for cytokinesis to occur properly. This inactivation is important to prevent Arp2/3 complex activation and its associated nucleation of branched actin network in HeLa cells, as previously shown in *C. elegans* (Canman *et al.*, 2008). Rac1 inactivation is also likely required to locally inhibit cell adhesion at the division plane, thus allowing for cytokinesis to occur properly (Bastos *et al.*, 2012). This idea is supported by the fact that depletion of Rac1 effectors known for their role in cell spreading and cell adhesion (i.e., PAK or ARHGEF7) also rescues the cytokinesis failure caused by MgcRacGAP depletion (Bastos *et al.*, 2012). It is possible that other Rac1 regulators or effectors will contribute to the rescue by releasing cell adhesion at the division plane subsequently, allowing efficient constriction of the contractile ring.

Finally, by identifying for the first time a GEF of Rac1 in dividing cells, this work adds insights to the complex picture of the role of MgcRacGAP in controlling RhoA and Rac1 during cytokinesis (Bement *et al.*, 2005; Piekny *et al.*, 2005; Yüce *et al.*, 2005; Loria *et al.*, 2012). Indeed, MgcRacGAP, which was initially characterized for its GAP activity on Rac1 in vitro (Touré *et al.*, 1998), has been described to control RhoA activity at the cleavage furrow (Jantsch-Plunger *et al.*, 2000; Bement *et al.*, 2005; Piekny *et al.*, 2005; Yüce *et al.*, 2005). In this regard, it is proposed that MgcRacGAP could activate RhoA via the regulation of the GEF Ect2 (Yüce *et al.*, 2005; Wolfe *et al.*, 2009; Loria *et al.*, 2012). By identifying Trio as a GEF controlling Rac1 activation in dividing cells, our work complements and strengthens recent studies in both vertebrate and invertebrate models, demonstrating that a crucial function for MgcRacGAP at the cleavage furrow is the inactivation of Rac1 (Canman *et al.*, 2008; Bastos *et al.*, 2012). Further work is required to test whether the Trio-Rac1 pathway in division is conserved in other systems.

MATERIALS AND METHODS

Cell culture, cell synchronization, and inhibitors

HeLa Kyoto cells were grown in DMEM (Life Technologies, Saint Aubin, France) supplemented with 10% fetal bovine serum, 2 mM L-glutamine, penicillin, and streptomycin (Life Technologies) at 37°C with 5% CO_2. To allow for anaphase enrichment (immunofluorescence experiments), cell synchronization was performed 6 h posttransfection. Cells were grown in the presence of 2 mM thymidine for 16 h and then released from the thymidine block and fixed 9 h later. To inhibit the Trio-Rac1 pathway, cells were treated for 24 h with 50 μM of ITX3, an inhibitor specific to Rac1 activation by Trio (Bouquier *et al.*, 2009). Control treatment with dimethyl sulfoxide (DMSO) was performed in parallel.

Transfection and cDNA

cDNA transfections were performed using JetPEI Transfection Reagent (Polyplus Transfection, Saint Quentin Yvelines, France) according to manufacturer's instructions for 24 h (GFP-Trio and Trio full-length mutants) or 48 h (GFP-DH1PH1). The GFP-DH1PH1 was previously described (Blangy *et al.*, 2000). Trio siRNA–resistant plasmids were subcloned using previously described GFP-Trio

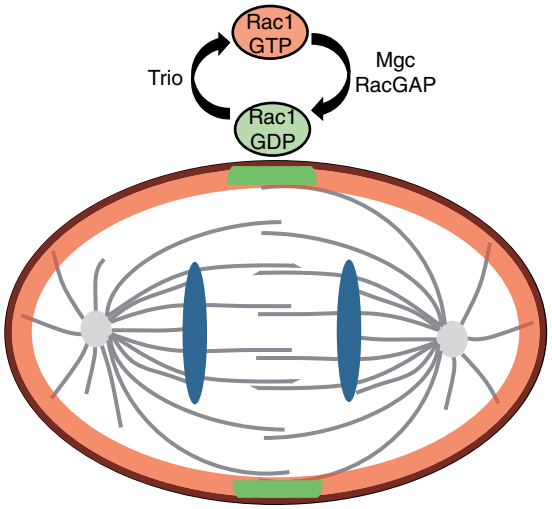

FIGURE 6: Model for Trio function in dividing cells. Trio functions as a GEF of Rac1 in dividing cells to control F-actin remodeling at the cell cortex. MgcRacGAP therefore counteracts the action of Trio by locally and temporally inhibiting Rac1 activation at the division plane, subsequently ensuring accurate cytokinesis.

constructs and include GFP Trio, GFP-D1d (unable to activate Rac1/RhoG), and GFP-D2d (unable to activate RhoA; Supplemental Figure S3; Bellanger *et al.*, 1998; Estrach *et al.*, 2002). Mutagenesis was performed using the QuikChange site-directed mutagenesis kit (Stratagene Agilent Technologies, Massy, France), according to manufacturer's instructions (cloning details can be obtained upon request). Oligonucleotides were ordered from Eurofins MWG Operon: Trio forward, 5′-GGTCAGCCAAGATGGGAAATCACTGCT AGACAAGCTCCAGCG-3′, and Trio reverse, 5′- CGCTGGAGCTT-GTCTAGCAGTGATTTCCCATCTTGGCTGACC-3′ (cloning details can be obtained upon request). All constructs were verified by sequencing. siRNA transfections were performed using Oligofectamine (Life Technologies) according to manufacturer's instructions. Trio, MgcRacGAP, Ect2, and Rac1 siRNA transfections were performed for 30 h unless otherwise specified. Arp3 siRNA transfections were performed for 72 h unless otherwise specified. The efficacy of protein depletion was assessed by immunoblotting and immunofluorescence posttransfection as indicated.

siRNA screening and siRNA sequences

HeLa cells were seeded in 96-well plates at a density of 2500 cells/well. At 24 h later, cells were transfected using Oligofectamine (Life Technologies) and 100 nM MgcRacGAP siRNA combined with 100 nM control, Rac1, or GEFs siRNA pools. At 48 h after transfection, cells were fixed in paraformaldehyde (PFA)-PHEM buffer (25 mM 4-(2-hydroxyethyl)-1-piperazineethanesulfonic acid [HEPES], 10 mM ethylene glycol tetraacetic acid, 60 mM 1,4-piperazinediethanesulfonic acid, 2 mM $MgCl_2$, pH 6.9) and stained with α-tubulin and 4′,6-diamidino-2-phenylindole (DAPI). Images were acquired (49 fields/well) using a Cellomics Arrayscan VTI HSCS reader (Thermo Scientific, Waltham, MA) equipped with a 20× objective (numerical aperture [NA] 0.4). siGENOME siRNA pools (screening) and individual siRNAs were purchased from Dharmacon (GE Healthcare, Lafayette, CO). Sequences are provided in Supplemental Table S1.

Antibodies

The following primary antibodies were used: Trio (DeGeer *et al.*, 2013), Western blot (WB), 1/1000; immunofluorescence (IF), 1/100; MgcRacGAP (Abcam, Paris, France; WB, 1/250; IF, 1/2000); α-tubulin (DM1alpha; Sigma-Aldrich, St. Louis, MO; WB, 1/400; IF, 1/200), fluorescein isothiocyanate–conjugated α-tubulin (DM1alpha; Sigma-Aldrich; IF, 1/500), Rac1 (BD Biosciences, Franklin Lakes, NJ; WB, 1/2000), rhodamine-phalloidin (Sigma-Aldrich; IF, 1/10,000), BCR (Cell Signaling, Danvers, MA; WB, 1/1000), β-Pix (gift from N. Morin; CRBM–CNRS, Montpellier, France; WB, 1/5000), GFP (Life Technologies; WB, 1/5000), p34-Arc/ARPC2 (Millipore, Molsheim, France; WB 1/5000), Phospho Histone H3 (Millipore; WB 1/5000), Ect2 (Santa Cruz C-20, Santa Cruz, CA; WB 1/1000), and DAPI (Cell Signaling; IF, 1/10 000). Secondary antibodies include, for IF, Alexa Fluor 488, 568, or 647–conjugated anti-rabbit or anti-mouse secondary antibodies (Molecular Probes, Carlsbad, CA; 1/1500) or 555–conjugated anti-goat (Jackson Immunoresearch, West Grove, PA; 1/500), and for WB, anti-mouse and anti-rabbit immunoglobulin G (IgG), horseradish peroxidase (HRP)–linked antibody (Cell Signaling; 1/2000) and anti-goat IgG, HRP-linked antibody (Jackson ImmunoResearch; 1/2000).

Immunofluorescence experiments, microscopy, and image analyses

Cells were fixed in 3.7% PFA in PHEM buffer containing 0.2% Triton X-100 for 15 min for actin staining or –20°C MeOH for microtubule staining. Then cells were blocked with 3% phosphate-buffered saline/bovine serum albumin and stained with the appropriate primary antibodies and secondary antibodies. Slides were mounted in Prolong Gold (Life Technologies). Multinucleated cell images were acquired with a Leica DM6000 microscope (40× objective; NA 1.25) controlled by MetaMorph (Molecular Devices, Downingtown, PA). Confocal images were acquired with a Leica SP5 confocal microscope with a 63× objective (NA 1.4). Fluorescence range intensity was adjusted identically for each series of panels. Image processing (cropping, rotating, brightness and contrast adjustment, and color combining) was performed with Imaris (Bitplane, St. Paul, MN) and Photoshop (Adobe). Images were assembled using Adobe Illustrator. Average intensity for actin staining was obtained from one *Z*-plane (lowest plane in focus) using MetaMorph.

Time-lapse imaging

Time-lapse imaging of cultured HeLa cells was performed using an inverted DMIRE2 Leica microscope equipped with a LMC Plan Fluor 40× objective (NA 0.55). Time-series images were acquired with a Micromax YHS 1300 4 (Roper Scientific, Tucson, AZ) controlled by MetaMorph. Time lapse was started 18 h after siRNA transfection, and images were taken every 6 min for 60 h. Time series of captured images were saved as .tiff files, which were compiled into .avi movies using ImageJ. Movies were displayed at 5 frames/s.

Lysates, gel electrophoresis, and immunoblotting

Cell lysates were obtained from HeLa cells 30 h after siRNA transfection. Lysis buffer: 20 mM HEPES, pH 7.0, 150 mM NaCl, 5 mM $MgCl_2$, 1% Triton X-100, and 1 μM protease inhibitor cocktail (Sigma-Aldrich, Hercules, CA). For the detection of BCR, urea buffer was used: urea 8 M in NH_4HCO_3 buffer, pH 7.5. Protein concentration was determined using Bio-Rad protein dye reagent (Bio-Rad Laboratories), loads were adjusted, and proteins were resolved by SDS–PAGE and analyzed by Western blot (Western Lightning Plus-ECL kit; PerkinElmer, Waltham, MA).

Rac1 activation assay

To assess Rac1 activity in mitosis, cell synchronization was achieved using double-thymidine block in HeLa cells (2 mM, 16 h). After 9 h

of release, cells (mitotic index count, 60%) were lysed in buffer containing 50 mM Tris-HCl (pH 7.5), 1% NP-40, 2 mM $MgCl_2$, 100 mM NaCl, 10% glycerol, 1 mM dithiothreitol, and 1 μM protease inhibitor cocktail. Protein lysates were subjected to centrifugation at 10,000 × *g* for 5 min at 4°C to remove insoluble materials. Endogenous GTP-Rac1 was pulled down by incubating the protein lysates for 1 h at 4°C with the Cdc42/Rac interactive binding domain (CRIB) of mouse PAK3 (amino acids 73–146) fused to glutathione *S*-transferase (GST) and coupled to glutathione–Sepharose beads (GE Healthcare). The beads were washed three times with lysis buffer and resuspended in SDS sample buffer. Protein samples were analyzed by Western blot using the anti-Rac1 antibody. The level of GTP-bound (active Rac1) protein was assessed using ImageJ and normalized to the total amount of Rac1 detected in the cell lysate.

Statistical analysis

The number of cells counted per experiment for statistical analysis is indicated in the figure legends. For graphs in all figures, error bars indicate mean of at least three independent experiments ± SEM unless otherwise specified. Statistical analyses were performed using Excel (Microsoft Redmond, WA) or Prism software (GraphPad, San Diego, CA). The *p* values were calculated using a two-tailed Student's *t* test. Graphs were created using Excel or Prism software.

ACKNOWLEDGMENTS

We thank Virginie Georget and Sylvain De Rossi for help and advice regarding microscopy and image analysis. The experiments reported here were performed within the France-BioImaging National Research Infrastructure at the MRI facility, Montpellier. France-BioImaging is supported by the French National Research Agency through the Investments for the Future Program (ANR-10-INSB-04). We also thank Christelle Anguille for help and advice in setting up the transfection conditions for the siRNA screening approach. This work was supported by the Fondation de France Comité Tumeurs, the Fondation ARC pour la Recherche sur le Cancer, and the Ligue contre le Cancer (Comité Régional Languedoc Roussillon; A.D.). A.C. was the recipient of a PhD Fellowship from the Ligue Nationale Contre le Cancer.

REFERENCES

Bastos RN, Penate X, Bates M, Hammond D, Barr FA (2012). CYK4 inhibits Rac1-dependent PAK1 and ARHGEF7 effector pathways during cytokinesis. J Cell Biol 198, 865–880.

Bateman J, Shu H, Van Vactor D (2000). The guanine nucleotide exchange factor trio mediates axonal development in the Drosophila embryo. Neuron 26, 93–106.

Bellanger JM, Lazaro JB, Diriong S, Fernandez A, Lamb N, Debant A (1998). The two guanine nucleotide exchange factor domains of Trio link the Rac1 and the RhoA pathways in vivo. Oncogene 16, 147–152.

Bement WM, Benink HA, von Dassow G (2005). A microtubule-dependent zone of active RhoA during cleavage plane specification. J Cell Biol 170, 91–101.

Blangy A, Vignal E, Schmidt S, Debant A, Gauthier-Rouvière C, Fort P (2000). TrioGEF1 controls Rac- and Cdc42-dependent cell structures through the direct activation of rhoG. J Cell Sci 113, 729–739.

Bouquier N, Vignal E, Charrasse S, Weill M, Schmidt S, Léonetti J-P, Blangy A, Fort P (2009). A cell active chemical GEF inhibitor selectively targets the Trio/RhoG/Rac1 signaling pathway. Chem Biol 16, 657–666.

Briançon-Marjollet A, Ghogha A, Nawabi H, Triki I, Auziol C, Fromont S, Piché C, Enslen H, Chebli K, Cloutier JF, *et al.* (2008). Trio mediates netrin-1-induced Rac1 activation in axon outgrowth and guidance. Mol Cell Biol 28, 2314–2323.

Canman JC, Lewellyn L, Laband K, Smerdon SJ, Desai A, Bowerman B, Oegema K (2008). Inhibition of Rac by the GAP activity of centralspindlin is essential for cytokinesis. Science 322, 1543–1546.

D'Avino PP, Glover DM (2009). Cytokinesis: mind the GAP. Nat Cell Biol 11, 112–114.

DeGeer J, Boudeau J, Schmidt S, Bedford F, Lamarche-Vane N, Debant A (2013). Tyrosine phosphorylation of the Rho guanine nucleotide exchange factor Trio regulates netrin-1/DCC-mediated cortical axon outgrowth. Mol Cell Biol 33, 739–751.

Estrach S, Schmidt S, Diriong S, Penna A, Blangy A, Fort P, Debant A (2002). The human Rho-GEF trio and its target GTPase RhoG are involved in the NGF pathway, leading to neurite outgrowth. Curr Biol 12, 307–312.

Hirose K, Kawashima T, Iwamoto I, Nosaka T, Kitamura T (2001). MgcRacGAP is involved in cytokinesis through associating with mitotic spindle and midbody. J Biol Chem 276, 5821–5828.

Jaffe AB, Hall A (2005). RHO GTPASES: biochemistry and biology. Annu Rev Cell Dev Biol 21, 247–269.

Jantsch-Plunger V, Gönczy P, Romano A, Schnabel H, Hamill D, Schnabel R, Hyman AA, Glotzer M (2000). CYK-4: A Rho family gtpase activating protein. (GAP) required for central spindle formation and cytokinesis. J Cell Biol 149, 1391–1404.

Jordan SN, Canman JC (2012). Rho GTPases in animal cell cytokinesis: an occupation by the one percent. Cytoskeleton 69, 919–930.

Li Y, Guo Z, Chen H, Dong Z, Pan ZK, Ding H, Su S-B, Huang S (2011). HOXC8-dependent cadherin 11 expression facilitates breast cancer cell migration through Trio and Rac. Genes Cancer 2, 880–888.

Loria A, Longhini KM, Glotzer M (2012). The RhoGAP domain of CYK-4 has an essential role in RhoA activation. Curr Biol 22, 213–219.

Moshfegh Y, Bravo-Cordero JJ, Miskolci V, Condeelis J, Hodgson L (2014). A Trio-Rac1-Pak1 signalling axis drives invadopodia disassembly. Nat Cell Biol 16, 574–586.

Newsome TP, Schmidt S, Dietzl G, Keleman K, Åsling B, Debant A, Dickson BJ (2000). Trio combines with Dock to regulate Pak activity during photoreceptor axon pathfinding in Drosophila. Cell 101, 283–294.

Piekny A, Werner M, Glotzer M (2005). Cytokinesis: welcome to the Rho zone. Trends Cell Biol 15, 651–658.

Pollard TD (2007). Regulation of actin filament assembly by Arp2/3 complex and formins. Annu Rev Biophys Biomol Struct 36, 451–477.

Rossman KL, Der CJ, Sondek J (2005). GEF means go: turning on RHO GTPases with guanine nucleotide-exchange factors. Nat Rev Mol Cell Biol 6, 167.

Schmidt A, Hall A (2002). Guanine nucleotide exchange factors for Rho GTPases: turning on the switch. Genes Dev 16, 1587–1609.

Seguin L, Liot C, Mzali R, Harada R, Siret A, Nepveu A, Bertoglio J (2009). CUX1 and E2F1 regulate coordinated expression of the mitotic complex genes Ect2, MgcRacGAP, and MKLP1 in S phase. Mol Cell Biol 29, 570–581.

Steffen A, Faix J, Resch GP, Linkner J, Wehland J, Small JV, Rottner K, Stradal TE B (2006). Filopodia formation in the absence of functional WAVE- and Arp2/3-complexes. Mol Biol Cell 17, 2581–2591.

Steven R, Kubiseski TJ, Zheng H, Kulkarni S, Mancillas J, Ruiz Morales A, Hogue CW, Pawson T, Culotti J (1998). UNC-73 activates the Rac GTPase and is required for cell and growth cone migrations in C. elegans. Cell 92, 785–795.

Touré A, Dorseuil O, Morin L, Timmons P, Jégou B, Reibel L, Gacon G (1998). MgcRacGAP, a new human GTPase-activating protein for Rac and Cdc42 similar to Drosophila rotundRacGAP gene product, is expressed in male germ cells. J Biol Chem 273, 6019–6023.

Van Rijssel J, Hoogenboezem M, Wester L, Hordijk PL, Van Buul JD (2012). The N-terminal DH-PH domain of Trio induces cell spreading and migration by regulating lamellipodia dynamics in a Rac1-dependent fashion. PLoS One 7, e29912.

Wolfe BA, Takaki T, Petronczki M, Glotzer M (2009). Polo-like kinase 1 directs assembly of the HsCyk-4 RhoGAP/Ect2 RhoGEF complex to initiate cleavage furrow formation. PLoS Biol 7, e1000110.

Yoshizaki H, Ohba Y, Kurokawa K, Itoh RE, Nakamura T, Mochizuki N, Nagashima K, Matsuda M (2003). Activity of Rho-family GTPases during cell division as visualized with FRET-based probes. J Cell Biol 162, 223–232.

Yoshizaki H, Ohba Y, Parrini M-C, Dulyaninova NG, Bresnick AR, Mochizuki N, Matsuda M (2004). Cell type-specific regulation of RhoA activity during cytokinesis. J Biol Chem 279, 44756–44762.

Yüce O, Piekny A, Glotzer M (2005). An ECT2-centralspindlin complex regulates the localization and function of RhoA. J Cell Biol 170, 571–582.